



International Journal of Pharmacology

ISSN 1811-7775

science
alert

ansinet
Asian Network for Scientific Information



Research Article

Neuroprotective Effects of Picroside II on Rats Following Cerebral Ischemia Reperfusion Injury by Inhibiting p53 Signaling Pathway

¹Tingting Wang, ¹Shan Li, ²Li Zhao and ¹Yunliang Guo

¹Institute of Cerebrovascular Diseases, Affiliated Hospital of Qingdao University, Taishan Scholars Construction Project Excellent Innovative Team of Shandong Province, 266003 Qingdao, China

²Department of Rehabilitation, Binzhou Medical University Hospital, 256600 Binzhou, China

Abstract

Background and Objective: Acute cerebral ischemia was caused by cerebral artery blockage, which was the most common type of cerebral ischemia and the second leading fatal disease. The aim of the current study was to analyze the effects of picroside II on brain tissues in rats following middle cerebral artery occlusion/reperfusion (MCAO/R). **Materials and Methods:** Healthy adult male Wistar rats were used to establish MCAO/R models by intraluminal thread methods. The experimental rats were randomly divided into sham, model, picroside II (Picr) and PET- α (Pifithrin- α hydrobromide, an inhibitor of p53) groups. The neurological deficit and infarct volume were assessed using mNSS test and TTC staining. The morphology and structure of cortical brain tissues were observed by Hand E and transmission electron microscopy (TEM). Apoptosis was counted by TUNEL. Mitochondrial permeability transition pore (mPTP) was determined using spectrophotometer. The expressions of p-p53, Bcl-2, Bax, Cyt c and Caspase-3 were tested using WB. **Results:** Picroside II ameliorated the neurological dysfunction of MCAO/R rats, reduced the cerebral infarct volume and apoptosis accompanied by mPTP closing and the inhibition of p53 signaling pathway and PET- α also simulated the therapeutic effect by inhibiting p53 signaling pathway. **Conclusion:** It was concluded that the MCAO/R could activate the opening of mPTP and neuronal apoptosis by p53 signaling pathway in rats. Picroside II played a neuroprotective role in inhibiting the activation of p53 signaling pathway.

Key words: Picroside II, cerebral ischemia-reperfusion injury, p53 signaling pathway, apoptosis, mPTP

Citation: Tingting Wang, Shan Li, Li Zhao and Yunliang Guo, 2019. Neuroprotective effects of picroside II on rats following cerebral ischemia reperfusion injury by inhibiting p53 signaling pathway. *Int. J. Pharmacol.*, 15: 790-800.

Corresponding Authors: Li Zhao, Department of Rehabilitation, Binzhou Medical University Hospital, 256600 Binzhou, China Tel: +8613012728510
Yunliang Guo, Institute of Cerebrovascular Diseases, Affiliated Hospital of Qingdao University, Taishan Scholars Construction Project Excellent Innovative Team of Shandong Province, 266003 Qingdao, China Tel: +8618661803619

Copyright: © 2019 Tingting Wang *et al.* This is an open access article distributed under the terms of the creative commons attribution License, which permits unrestricted use, distribution and reproduction in any medium, provided the original author and source are credited.

Competing Interest: The authors have declared that no competing interest exists.

Data Availability: All relevant data are within the paper and its supporting information files.

INTRODUCTION

Acute cerebral ischemia was caused by cerebral artery blockage, which was the most common type of cerebral ischemia, accounting for more than 80% of all cerebral ischemia¹. When cerebral ischemia occurred, cerebral blood flow (CBF) decreased sharply and the damage diffused from the center to the periphery but ischemic penumbra (IP), outside of the ischemic core, was still hypoperfusion, CBF maintained² at 7~17 mL/100 g min⁻¹. The cerebral ischemic penumbra depended on the collateral circulation of the brain and no irreversible death occurred in the neurons. Therefore, after reperfusion, the neurons could still survive and recover their function³. Therefore, in most cases, timely thrombolytic therapy was essential for the treatment of acute ischemic stroke. However, the inflammatory injury, oxidative stress, excitatory amino acid toxicity and apoptosis caused by reperfusion were the key problems affecting the recovery of cerebral ischemia⁴. So, the discovery of important signaling molecules and related signal pathways to protect neurons in the ischemic penumbra was beneficial to the formulation of neuroprotective treatment strategies.

The p53 tumour suppressor was one of the major signaling pathways of apoptosis. The p53 protein was a nuclear transcription factor⁵ that regulated the expression of a wide variety of genes involved in apoptosis, growth arrest or senescence in response to genotoxic or cellular stress⁵. Recent studies found that p53 was also widely associated with the occurrence and development of stroke^{6,7} and Alzheimer's disease⁸. For example, p53 mediated neuronal death after cerebral ischemia-reperfusion injury through Bax/Cytochrome c/caspases⁹.

Mitochondrial permeability transition pore (mPTP) has consisted of voltage-dependent anion channel (VDAC), adenine translocase (ANT), cyclosporin A-binding protein D (Cyp D) and some other molecules¹⁰. Mitochondrial membrane permeability transition, which occurred at the apoptotic stage, was recognized as a key event in cell death¹¹. Firstly, some extracellular signals or DNA damage in cells activated apoptotic members of the Bcl-2 family, such as Bax or Bak, thus transferring from cytoplasm to mitochondrial membrane, making mPTP open and mitochondrial transmembrane potential decrease and finally apoptotic signaling molecules such as cytochrome c, entering the cytoplasm, activating caspase-3 and leading to apoptosis¹².

Picroside II was an iridoid terpenoid compound, which was one of the main active components of Huanglian. Research group found that picroside II exerted a neuroprotective effect by inhibiting the mitochondria Cyt c

signal pathway following ischemia reperfusion injury in rats¹³; however, the specific mechanism related to the working of picroside II and its ability to inhibit the apoptosis via p53 signaling pathway remained unclear. Therefore, this study attempted to investigate the neuroprotective effect of picroside II on cerebral ischemia reperfusion injury (middle cerebral artery occlusion/reperfusion, MCAO/R) in rats and its relationship with p53 signaling pathway.

MATERIALS AND METHODS

All the work related to this study was conducted in affiliated institutes. The analytical part and animal study was conducted from 2017.01-2018.12 and other work was completed on 2019.01.

Drugs and chemicals: Picroside II, CAS No. 39012-20-9, purity>98%, molecular formula: C₂₃H₂₈O₁₃, molecular weight: 512, Tianjin Kuiqing Medical Tech. Co. Ltd.; Pifithrin- α hydrobromide, inhibitor of p53, CAS No. 63208-82-2, purity 98.14%, molecular formula: C₁₆H₁₉BrN₂OS, molecular weight: 367.30, Selleck, USA; Tissue mitochondrial isolation kit (C3606) and enhance BCA protein assay kit (P0010) Beyotime Biotechnology, China; *in situ* cell death detection kit, Fluorescein, 11684795910, Roche, USA; p-p53 rabbit polyclonal antibody, ab1431, abcam, USA; p53 rabbit monoclonal antibody, 32532, CST, USA; Bcl-2 rabbit polyclonal antibody, 12789-1-AP, Bax rabbit polyclonal antibody, 50599-2-Ig, COXIV rabbit Polyclonal antibody, 11242-1-AP, Proteintech, USA; Cyt c rabbit antibody, ab18738, caspase-3 rabbit antibody, ab13847, Abcam, USA; β -actin rabbit antibody, bs-0061R, bioss, Beijing; goat anti-rabbit IgG (H+L), HP conjugate, SA00001-2, Proteintech, USA. The other chemicals like KCL, CaCl₂ were purchased from Aladdin, (Shanghai) China (Analytical Grade).

Animal models: In total, 120 healthy adult male SPF-grade Wistar rats weighing 220-250 g were provided by the Experimental Animal Centre of Jinan Pengyue (SCXK (LU) 20140007). The animals were housed at the ambient temperature of 25°C with natural illumination and free access to food and water for seven days to adapt to the environment. All animal-related experiments were performed using the protocols approved by the Ethics Committee of Qingdao University Medical College (QUMC 2015-09). Experimental MCAO 2 h/R 22 h models were made by intraluminal monofilament suture in the left external-internal carotid artery¹⁴. After reperfusion, the neurobehavioral function of the rats was evaluated by a modified neurological severity

score (mNSS) test¹³. Rats with an mNSS score ranging from 7-12 were considered successful models and rats were randomly divided in order to separate groups (n = 20)^{13,15}. Details of groups given:

- **Sham group:** The rats underwent the same surgical procedure without the insertion of the thread embolism into the MCA and received saline 0.5 mL before reperfusion
- **Model group:** The MCAO 2 h/R 22 h model was established and the suture was removed synchronously peritoneal injection¹³ saline 0.5 mL
- **Picr group:** The model was made as a model group. Picoside II was diluted in a normal saline solution and the rats was treated with picoside II (20 mg kg⁻¹) by peritoneal injection before reperfusion¹³
- **PET- α group:** The model was made as model group. PET- α was diluted in normal saline solution containing 2% DMSO and the rats were treated with PET- α (2.2 mg kg⁻¹) by peritoneal injection before MCAO¹⁶

Evaluation index

Neurobehavioral function evaluation: An observer blind to the experimental groups evaluated the neurobehavioral function of each rat before and 22 h after reperfusion by the mNSS test.

TTC staining: At MCAO 2 h/R 22 h, 5 rats were dissected and their brains were removed immediately. The cerebral infarct volume (CIV) were processed and determined according to the method described by Zhang *et al.*¹³. The CIV was presented as a percentage of the infarct area/the ipsilateral hemisphere area at the coronal section of the optic chiasma¹³.

HE staining: At MCAO 2 h/R22 h, 5 rats were dissected and their brains were removed immediately. The histological changes were observed according to the method described by Wang *et al.*¹⁷ and Zhao *et al.*¹⁸. Four non-overlapping views of the cortex in each slice were randomly captured under a microscope (Leica DMI400, Germany) at 400-fold magnification to count the number of denatured cells^{17,18}.

TUNEL: The TUNEL staining was performed by strictly following the manufacturer's instructions. Under a 200-fold immune fluorescence microscope, the apoptotic cells exhibited green fluorescence and the cells showed blue fluorescence. Images of 4 non-overlapping views in the cortex were captured to calculate the apoptotic cell index:

$$ACI = \frac{\text{Number of apoptotic cells}}{\text{Total cells}}$$

The ACI indicated the degree of apoptosis.

Transmission electron microscopy (TEM): At MCAO 2 h/R 22 h, we randomly selected 5 rats per group. The ultra thin slices were made according to Zhao *et al.*¹⁹. The ultrastructure of the neurons was observed by TEM (JEM-1200EX, Japan).

MPTP permeability: The remaining 100 mg of fresh tissue as noted above was rapidly placed in a 1.5 mL EP tube. The MPTP openness was performed and detected by Li *et al.*²⁰, which presented as changes in absorbance (ΔS) after reaching equilibrium.

Subcellular fraction: About 22 h after reperfusion, the rats were anesthetized and reperused with 200 mL saline from the heart into the aorta. About 100 mg of fresh ischemic brain tissue from each group was washed with PBS and placed into EP tubers. The mitochondrial protein and cytoplasmic protein were extracted according to the manual for tissue mitochondria isolation kit. The protein concentrations were determined using BCA protein assay kit.

Western blot (WB) analysis: At MCAO 2 h/R 22 h, there were five rats left in per group. Protein extraction and WB were performed according to Zhang *et al.*¹³. The grey value of each band was measured using Quantity One software. The relative value of the protein (RVP) is the grey value of the target protein/the grey value of β -actin¹³. The experiment was repeated 5 times and the results are presented as the mean \pm SD.

Statistical analysis: The SPSS 22.0 software was used for the statistical analysis. One-way analysis of variance (one-way ANOVA) was used for the multi-group comparisons. Bonferroni tests were used for two-group comparisons. The values were considered significant at p-values less than 0.05.

RESULTS

Neurobehavioral function evaluation: The neurological function was graded using a scale from 0-18 (normal score, 0; maximal deficit score, 18) and higher the score indicated the heavier dysfunction. As shown in Table 1, the score in the sham group was 0. In the model group, the mNSS score increased to 9.2 ± 2.7 , which was statistically higher than

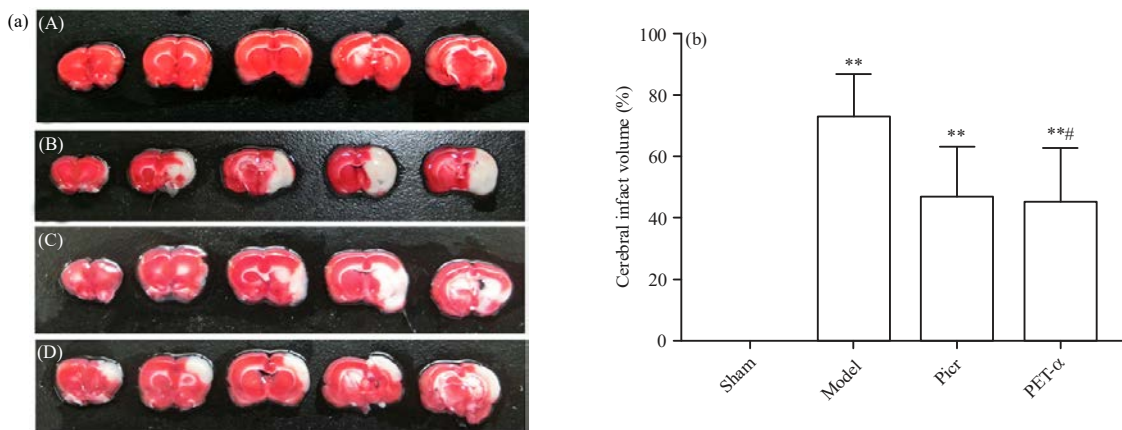


Fig. 1 (a-b): (a) TTC staining and (b) Statistical analysis of CIV in MCAO/R rats

A: Sham group, B: Model group, C: Picr group, D: PET-α group. **p<0.01 vs. Sham group, #p<0.05 vs. Model group, TTC: Triphenyltetrazolium chloride

Table 1: Scores of mNSS in MCAO/R rats

| Groups | Scores of mNSS |
|--------|----------------|
| Sham | 0 |
| Model | 9.2 ± 2.7* |
| Picr | 7.7 ± 1.0# |
| PET-α | 7.7 ± 1.4# |

*p<0.05 vs. Sham group, #p<0.05 vs. Model group

sham group ($t = 14.28, p < 0.01$). In the Picr and PET-α groups, mNSS score dropped to 7.7 ± 1.0 and 7.7 ± 1.4 which were statistically lower than model group ($t = 2.9, 2.9, p = 0.03$).

Cerebral infarct volume: The TTC staining revealed that in the sham group, the brain sections were uniformly red and there was no cerebral ischemic infarct (Fig. 1a), while large white infarct lesions were observed in the model group (CIV = 72.62 ± 14.39 , Fig. 1b). The CIV in the Picr group was (46.52 ± 16.94), which was much smaller than that in model group, but there was no significant difference between the two groups ($t = 2.87, p = 0.06$). The CIV in the PET-α group (44.76 ± 18.13) was significantly smaller than the model group ($t = 3.07, p < 0.05$).

Histological changes: Results in Fig. 2 showed the histological changes of neurons in the cortex of rats in different groups by HE staining. In the sham group the neurons were uniformly coloured with a complete structure and neat arrangement (Fig. 2a). In the model group, the neurons were wrinkled, the gap around the cells was increased, the nuclei were pyknotic and deeply stained, vacuoles were formed caused by dissolution of cells (Fig. 2b), denatured cells increased and almost no normal cells existed. In the Picr group, the neuronal injury was

mitigated and the cells were arranged neatly. Only a few cells were deeply stained with solid shrinkage (Fig. 2c). In the PET-α group the neuronal injury was close to Picr group. Normal cells and denatured cells coexisted and normal cells outnumbered denatured cells (Fig. 2d).

Neuronal ultrastructure: In the sham group, the cortical neurons had a clear outline, large and round nuclei and uniform chromatin (Fig. 3a). At a high magnification, a clear and complete double nuclear membrane was found and different organelles such as mitochondria and golgi apparatus were distributed in the cytoplasm (Fig. 3a). In the model group, the neuronal morphology was irregular, chromatin was condensed and the organelles were dissolved (Fig. 3b). At a high magnification, the double-layer nuclear membrane was blurred, many organelles in the cytoplasm were dissolved and disappeared and the mitochondria were swelled and deformed (Fig. 3b). Compared with model group, the damage of neuron in Picr group was much slighter and the structure of the neurons was intact (Fig. 3c). At a high magnification, the blurred double-layer nuclear membrane was observed and many organelles were scattered in the cytoplasm (Fig. 3c). In PET-α group, the damage to the neuron was similar to that in Picr group (Fig. 3d). At a high magnification, the double-layer nuclear membrane was unclear with some a few deformed and swelling mitochondria (Fig. 3d).

Neuronal apoptosis: The TUNEL staining showed (Fig. 4) that the apoptotic cells exhibited green fluorescence in the nuclei and the cells showed blue fluorescence (a1-d1). The apoptotic cell index (ACI = the number of apoptotic cells/total cells) was detected to indicated the degree of apoptosis and merge of

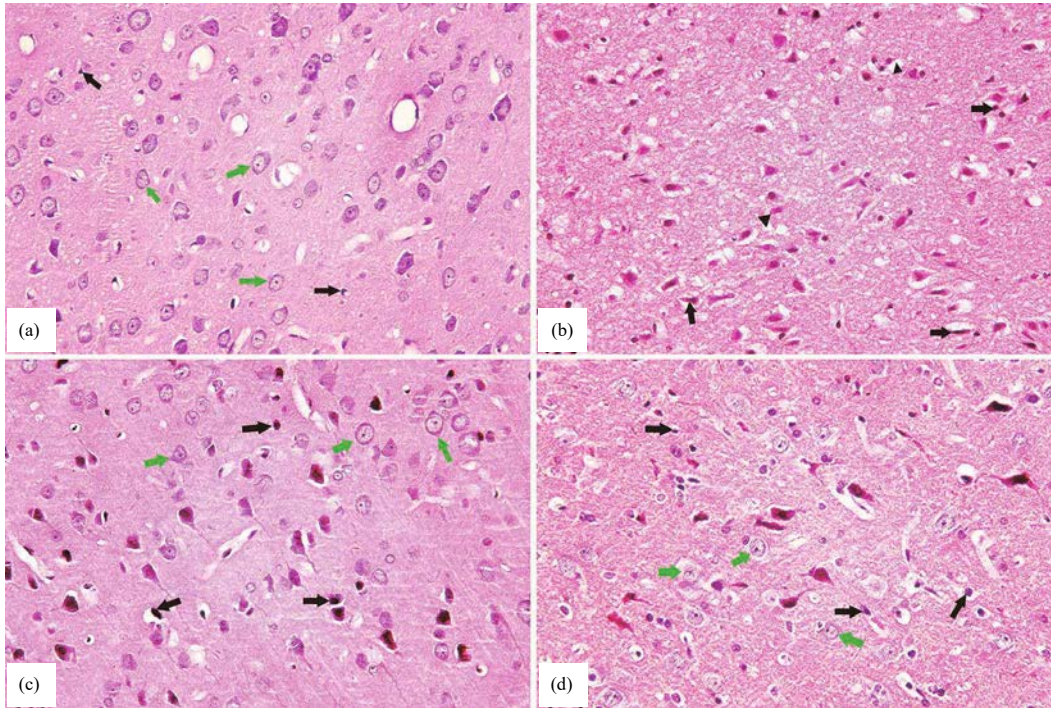


Fig. 2(a-d): Morphology of neurons in the cortex of rats by HE ×400

a: Sham group, b: Model group, c: Picr group, d: PET- α group. Black arrow stood for denatured cell, green arrow stood for normal cell, black triangle stood for vacuole

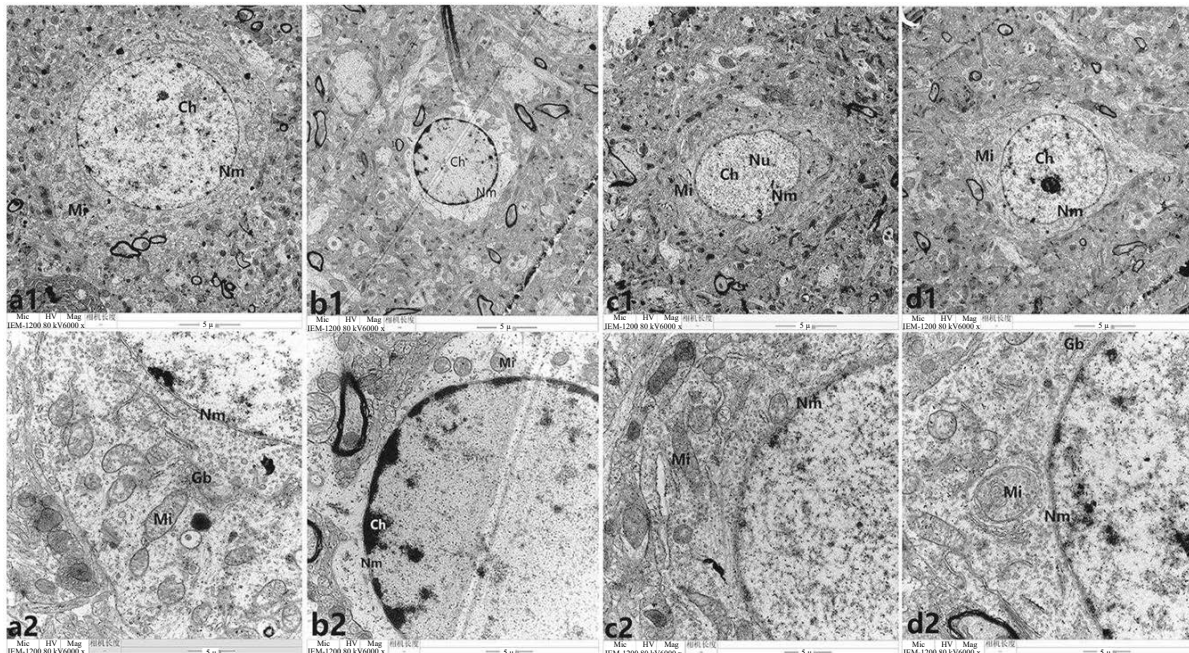


Fig. 3(a-d): Ultrastructure of neurons in the rat cortex by TEM, EM ×6K ×25K

a1: Sham group at 6000-fold magnification, a2: Sham group at 24000-fold magnification, b1: Model group at 6000-fold magnification, b2: Model group at 24000-fold magnification, c1: Picr group at 6000-fold magnification, c2: Picr group at 24000-fold magnification, d1: PET- α group at 6000-fold magnification, d2: PET- α group at 24000-fold magnification. Nu: Nucleolus, Nm: Nuclear membrane, Ch: Chromatin, Mi: Mitochondria, Gb: Golgi apparatus

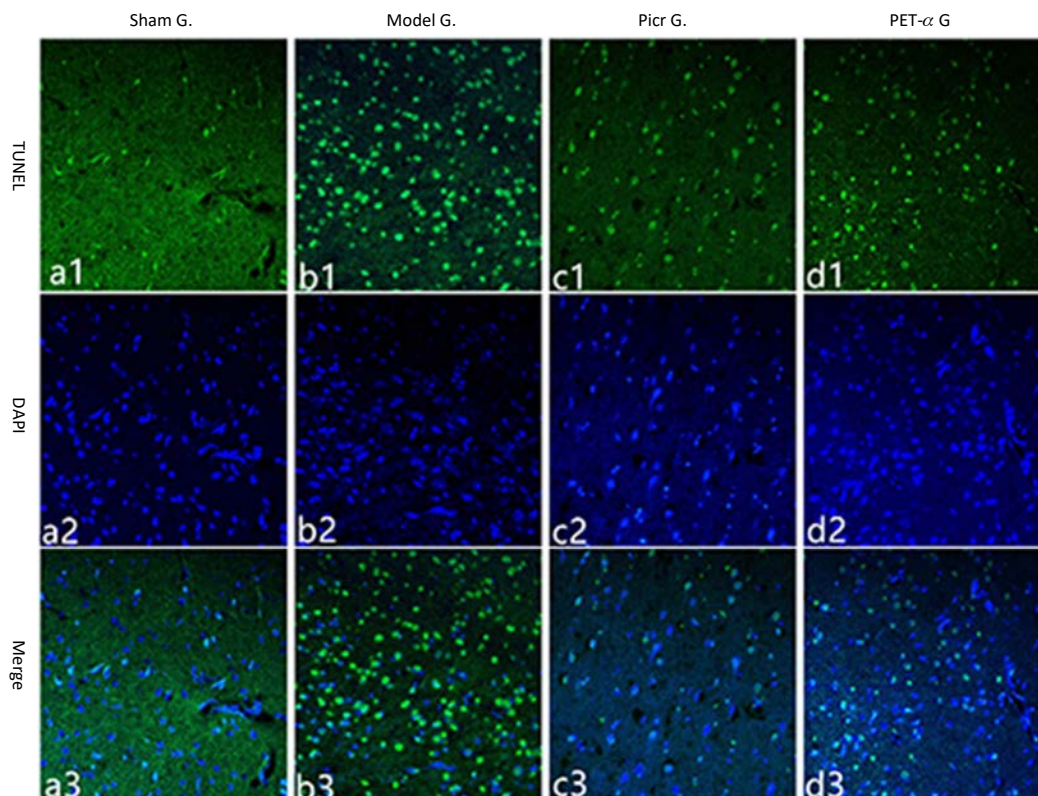


Fig. 4(a-d): Apoptosis of neuronal cells in each group by TUNEL $\times 200$

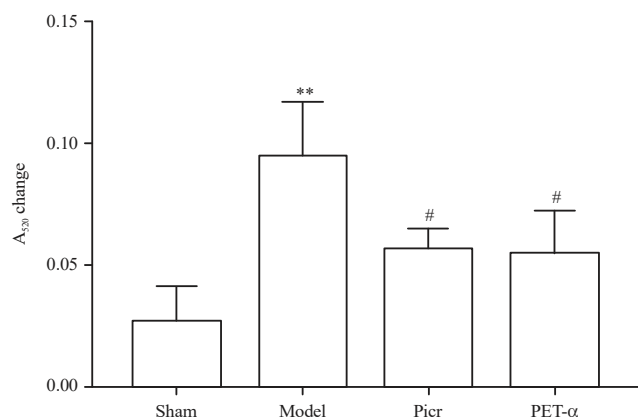


Fig. 5: Change in absorbance of A520

** $p < 0.01$ vs. Sham group, # $p < 0.05$ vs. Model group

results could reflect the ACI. In the model group, apoptotic cells were increased clearly and ACI = 0.684 ± 0.08 was increased significantly compared to sham group ($t = 6.02$, $p < 0.01$, Fig. 4b1 and b3). In the Picr group, apoptotic cells were reduced and ACI = 0.43 ± 0.14 was decreased significantly compared to sham group than model group

($t = 3.09$, $p = 0.04$, Fig. 4c1-c3). In PET- α group, the ACI = 0.478 ± 0.19 was close to that in Picr group ($t = 0.58$, $p > 0.05$, Fig. 4d1 and d3).

Opening of mPTP: As shown in Fig. 5, the change in absorbance of A520 in the model group was increased obviously compared with sham group ($t = 6.29$, $p < 0.01$). However, after treatment with Picr or PET- α , the change in absorbance of A520 was markedly lower than model group ($t = 3.51, 3.70$, $p < 0.05$).

Protein expressions

Expression of p-p53: The P53 tumor suppressor proteins played an important role in cellular responses to DNA damage and other genomic aberrations. Activation of p53 led to cell cycle arrest, DNA repair, or apoptosis²¹. The P53 was activated by phosphorylated at multiple sites (Ser15 or Ser20) *in vivo*²². So in this experiment, p53 without detecting any phosphorylated sites was detected to express total p53 including inactivated and activated p53 and phosphorylated p53 (p-p53) was detected to express the activated p53. The ratio of p-p53/p53 was

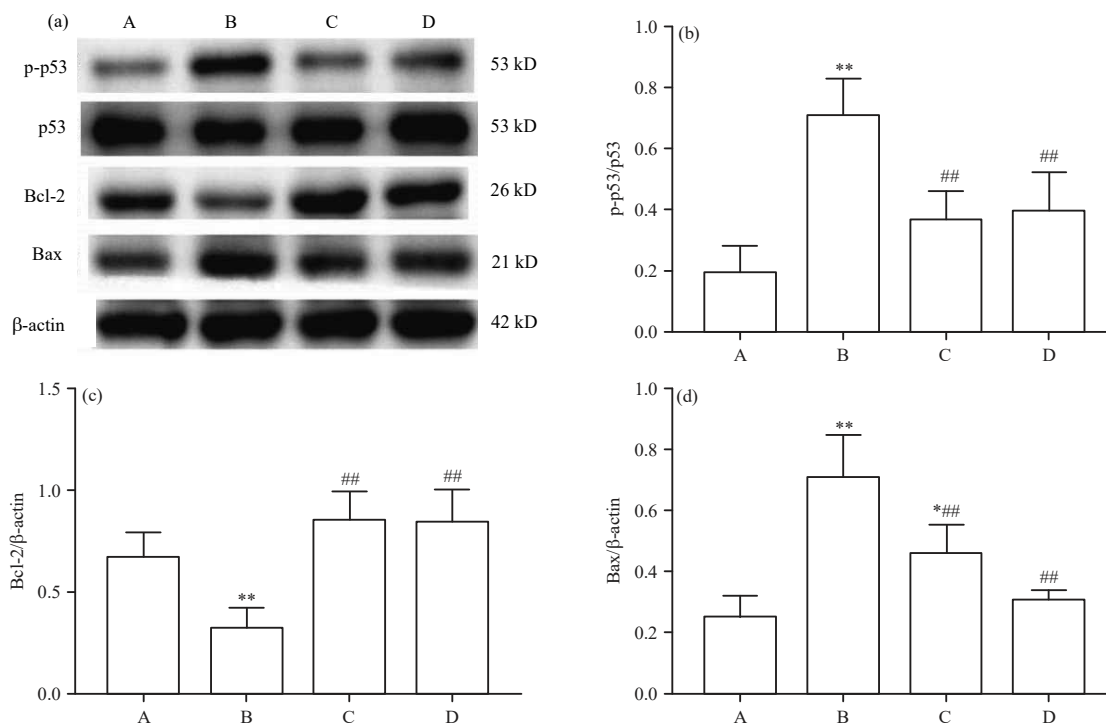


Fig. 6(a-d): Blots and statistical analyses of p-p53, Bcl-2 and Bax following MCAO/R

a: Blots of different proteins following MCAO/R, b: Blot analysis of p-p53, c: Blot analysis of Bcl-2 and d: Blot analysis of Bax, A: Sham group, B: Model group, C: Picr group, D: PET-α group, * $p < 0.05$ vs. Sham group, ** $p < 0.01$ vs. Sham group, ## $p < 0.01$ vs. Model group

accessed to indict the activation of p53. Data in Fig. 6a and 6b showed that p-p53 and p53 had a molecular weight of 53 kDa. The P-p53 was only weakly expressed in the sham group. Compared with sham group, the expression of p-p53 was increased to a great extent and the ratio was significantly higher in model group ($t = 7.18$, $p < 0.01$). In the Picr and PET-α groups, p-p53 expression was decreased and the ratio was significantly lower than model group ($t = 4.79$, 4.39 , $p < 0.01$).

Expressions of Bcl-2: Results in Fig. 6a and c showed that Bcl-2 had a molecular weight of 26 kDa and was strongly expressed in the sham group. In the model group, the expression of Bcl-2 was significantly lower compared with sham group ($t = 3.95$, $p < 0.01$). In the Picr and PET-α groups, Bcl-2 expression were at the same level ($t = 0.12$, $p > 0.05$) both of which were much higher than model group ($t = 6.13$, 6.02 , $p < 0.01$).

Expressions of Bax: Figure 6a and d showed that Bax had a molecular weight of 21 kDa and had a weak expression in the sham group. In the model group, the expression of Bax was significantly raised than sham group ($t = 7.46$, $p < 0.01$). In the Picr group, Bax expression was significantly lower than model group ($t = 4.11$, $p < 0.01$).

And in the PET-α group, Bax expression was further decreased and close to the level of sham group ($t = 0.92$, $p > 0.05$).

Expressions of Cyt c in mitochondria and cytoplasm: Results in Fig. 7 showed that Cyt c had a molecular weight of 11 kDa. As shown in Fig. 7a, Cyt c expression was strongly expressed in the sham group. In the model group, the expression of Cyt c was significantly lower compared with sham group ($t = 6.67$, $p < 0.01$). While in the Picr and PET-α groups, Cyt c expression was significantly increased than model group ($t = 3.50$, 3.47 , $p < 0.05$).

As shown in Fig. 7b, Cyt c expression was the opposite that in mitochondria. Cyt c expression was weakly expressed in the sham group. In the model group, the expression of Cyt c was much increased than sham group ($t = 7.69$, $p < 0.01$). In the Picr and PET-α groups, Cyt c expression was much lower than model group ($t = 5.37$, 5.54 , $p < 0.05$).

Expressions of caspase-3: Figure 8 showed that caspase-3 expression was weakly expressed in the sham group. In the model group, the expression of caspase-3 was obviously higher than sham group ($t = 11.27$, $p < 0.01$). In the Picr and PET-α groups, caspase-3 expression was much lower than model group ($t = 7.07$, 7.92 , $p < 0.01$).

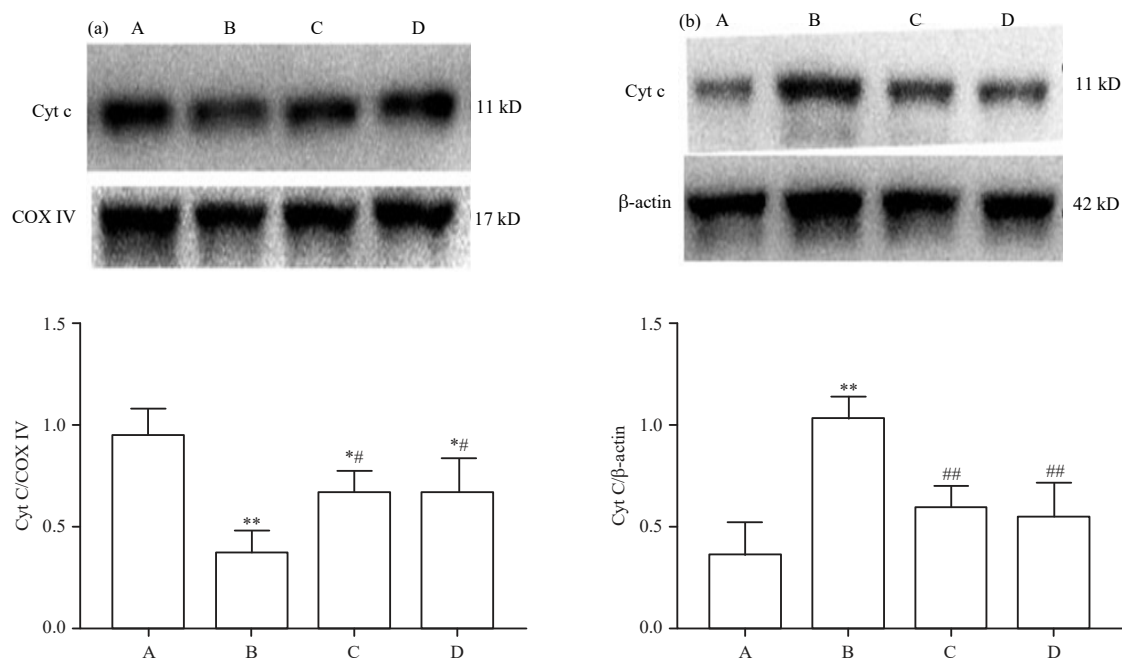


Fig. 7(a-b): Blots and statistical analysis of Cyt c in mitochondria and cytoplasm following MCAO/R
a: Blot and analysis of Cyt c in mitochondria following MCAO/R and b: Blot and analysis of Cyt c in cytoplasm following MCAO/R, A: Sham group, B: Model group, C: Picr group, D: PET- α group, * $p < 0.05$ vs. Sham group, ** $p < 0.01$ vs. Sham group, # $p < 0.05$ vs. Model group, ## $p < 0.01$ vs. Model group

DISCUSSION

In this experiment, the results showed that MCAO/R could activate the p53 signaling pathway to induce apoptosis while picoside II could inhibit the activation of p53 signaling pathway to reduce the cerebral ischemia-reperfusion injury. In this experiment, a common ischemic stroke MCAO/R model was preferred as it resembled most of the pathophysiological features of stroke^{23,24}. To evaluate the neuroprotective effect of picoside II, the neurobehavioral function score, infarct volume and histological changes and ultrastructure of neurons were observed following MCAO/R induction. The neurobehavioral function score and cerebral infarct volume were significantly increased ($p < 0.01$) with severe injury in histological changes and ultrastructure of neurons in model group due to MCAO/R-induced brain damage via apoptosis generation. The results are in corroboration with the studies of Li *et al.*²⁵. Treatment with Picoside II following MCAO/R in rats, would improve the neurological function of rats and lower cerebral infarct volume by inhibiting neuronal apoptosis²⁵. Moreover, Wu *et al.*²⁶ indicated that treatment with 10 and 100 μ M picoside II significantly improved postischemic myocardial function, reduced myocardial infarct size and inhibited apoptosis in myocardial ischemia reperfusion injury rats.

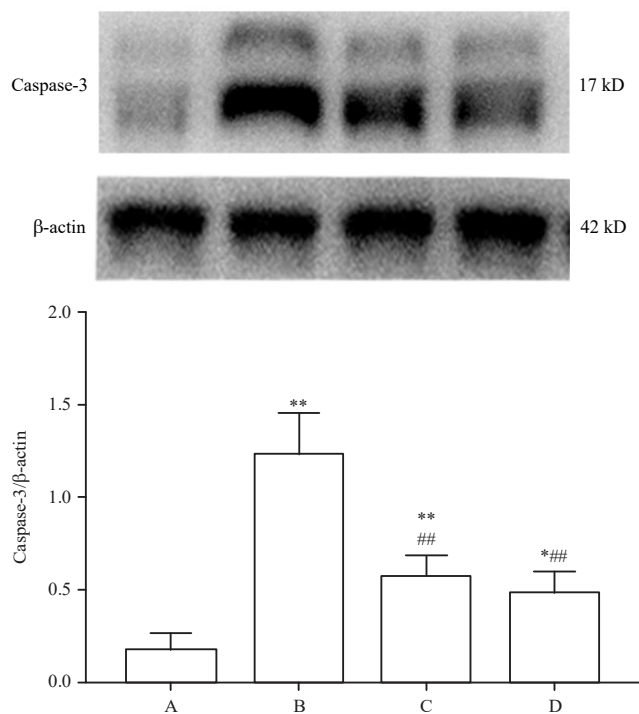


Fig. 8: Blot and statistical analysis of caspase-3 following MCAO/R
A: Sham group, B: Model group, C: Picr group and D: PET- α group, * $p < 0.05$ vs. Sham group, ** $p < 0.01$ vs. Sham group, ## $p < 0.01$ vs. Model group

During apoptosis, mitochondrial membrane permeability increased, partly owing to the opening of mPTP, a multiprotein complex built up at the contact site between the inner and the outer mitochondrial membranes²⁷. The mPTP has been previously implicated in clinically relevant massive cell death induced by toxins, anoxia, reactive oxygen species and calcium overload²⁷. Li *et al.*²⁰ showed that MCAO/R induced injury could induce apoptosis via upregulating the expression of VDAC1 and increasing the permeability of mPTP and picoside II could inhibit the apoptosis by decreasing the permeability of mPTP. In this experiment, in model group, the change in absorbance of A520 was markedly increased, which indicated the degree of mPTP openness increased. But after treatment with picoside II, the change in absorbance of mPTP in the Picr group was significantly lower than that in the model group ($p < 0.05$), implying that picoside II could inhibit the openness of mPTP, which was consistent with previous results. Multiple mitochondrial outer membrane apoptotic stresses led to opening of the mPTP, which resulted in the release of apoptotic factors including Cyt c, Endo G and AIF²⁸. In the cytosol, Cyt c mediated the allosteric activation of apoptosis-protease activating factor 1, which was required for the proteolytic maturation of caspase-9 and caspase-3. Activated caspases ultimately led to apoptosis²⁹. In this experiment, the release of Cyt c in cytoplasm and caspase-3 expression was increased in model group. However, in Picr group, the release of Cyt c in cytoplasm and caspase-3 expression was decreased. The results were in corroboration with the studies of Zhang *et al.*¹³. It was found that after MCAO/R, the expression of Cyt c and caspase-3 was increased to induce apoptosis and picoside II exerted a neuroprotective effect by inhibiting the mitochondria Cyt c signal pathway following ischemia reperfusion injury in rats. It was suggested that picoside II could inhibit the Cyt c release via inhibiting the openness of mPTP.

In order to further explore that how picoside II inhibited the openness of mPTP, p53 was detected. In brain, p53 was a major mediator of ischemia-induced cell death³⁰. Previous studies reported that p53 could be activated to mediate neuronal death during cerebral ischemia reperfusion injury. Treatment with PFT- α (the specific inhibitor of p53) 6, 30 min before or 1 h following MCAO could reduce p53 activity, apoptotic cells, cerebral infarct volume in the ischemic brain and motor disability in rats^{31,32}. It was reported that p53 induced apoptosis through p53 translocation to mitochondria³³. According to previous report, its translocation could directly activate pro-apoptotic Bcl-2 family members such as Bax and Bak, leading to apoptosis^{34,35}. Most of Bax were located in cytoplasm in the form of monomers.

Activated Bax could form oligomers, transferred from the cytoplasm to the mitochondrial membrane, formed a polymer with Bcl-2, triggered the openness of the mPTP and finally led to the release of Cyt c^{34,35}. In this experiment, the results showed that in model group, along with an increase in p-p53 and Bax and a decrease in Bcl-2 following MCAO/R. However, in PET- α group, the activation of p53 and Bax was inhibited and apoptotic cells were reduced with the closing of mPTP, which was similar to the treatment effect of Picr group. It was suggested that cerebral ischemia-reperfusion injury could induce apoptosis via activating p53 signaling pathway to open mPTP. And in Picr group, the inhibition of p53 and Bax was also observed, indicating that picoside II could down-regulate p53 signaling pathway following MCAO/R to inhibit apoptosis. In this study, the effect of picoside II on MCAO/R rats via p53 signaling pathway was only observed and its specific mechanism needed further validation in follow-up experiment.

CONCLUSION

The experiment indicated that cerebral ischemia reperfusion injury could induce apoptosis via activating p53-Bax/Bcl-2/Cyt c/caspase 3 signaling pathway. And treatment with picoside II could inhibit apoptosis, reduce the cerebral infarct volume and improve the neurobehavioral function in rats by down-regulating p53 signaling pathway following MCAO/R in rats to protect nervous system.

SIGNIFICANCE STATEMENT

This study discovered the mechanism of picoside II on cerebral ischemia that could be beneficial for other scientist to explore the neuroprotective effects of picoside II. This study will help the researchers to uncover the critical areas of Chinese medicine for stroke that many researchers were not able to explore. Thus a new theory on Chinese medicine for stroke may be arrived at.

ACKNOWLEDGMENTS

This experiment was supported by grant-in-aids for the Natural Science Fund of China (81274116), Qingdao Municipal Fund of Science and Technology (18-6-1-84-nsh), the Clinical Medicine+X Project Fund of Qingdao University Medical College (2017M032), Natural Science Fund of Shandong (ZR2014HP067, ZR2019MP009) and Qingdao traditional Chinese medicine scientific research program (2019-zyy066).

REFERENCES

1. Moskowitz, M.A., E.H. Lo and C. Iadecola, 2010. The science of stroke: Mechanisms in search of treatments. *Neuron*, 67: 181-198.
2. Ji, Y., L. Teng, R. Zhang, J. Sun and Y. Guo, 2017. NRG-1 β exerts neuroprotective effects against ischemia reperfusion-induced injury in rats through the JNK signaling pathway. *Neuroscience*, 362: 13-24.
3. Jackman, K. and C. Iadecola, 2015. Neurovascular regulation in the ischemic brain. *Antioxid. Redox. Signal.*, 22: 149-160.
4. Nielsen, M.M., K.L. Lambertsen, B.H. Clausen, M. Meyer and D.R. Bhandari *et al.*, 2016. Mass spectrometry imaging of biomarker lipids for phagocytosis and signalling during focal cerebral ischaemia. *Scient. Rep.*, Vol. 6. 10.1038/srep39571.
5. Laptenko, O. and C. Prives, 2006. Transcriptional regulation by p53: One protein, many possibilities. *Cell Death Differ.*, 13: 951-961.
6. Irminger-Finger, I., W.C. Leung, J. Li, M. Dubois-Dauphin and J. Harb *et al.*, 2001. Identification of BARD1 as mediator between proapoptotic stress and p53-dependent apoptosis. *Mol. Cell*, 8: 1255-1266.
7. Vaseva, A.V., N.D. Marchenko, K. Ji, S.E. Tsirka, S. Holzmann and U.M. Moll, 2012. p53 opens the mitochondrial permeability transition pore to trigger necrosis. *Cell*, 149: 1536-1548.
8. Savica, R., T.G. Beach, J.G. Hentz, M.N. Sabbagh and G.E. Serrano *et al.*, 2019. Lewy body pathology in Alzheimer's disease: A clinicopathological prospective study. *Acta Neurol. Scand.*, 139: 76-81.
9. Xie, Y.L., B. Zhang and L. Jing, 2018. MiR-125b blocks bax/cytochrome C/caspase-3 apoptotic signaling pathway in rat models of cerebral ischemia-reperfusion injury by targeting p53. *Neurol. Res.*, 40: 828-837.
10. Perez, M.J. and R.A. Quintanilla, 2017. Development or disease: Duality of the mitochondrial permeability transition pore. *Dev. Biol.*, 426: 1-7.
11. Zhan, M., C. Brooks, F. Liu, L. Sun and Z. Dong, 2013. Mitochondrial dynamics: Regulatory mechanisms and emerging role in renal pathophysiology. *Kidney Int.*, 83: 568-581.
12. Martinou, J.C., S. Desagher and B. Antonsson, 2000. Cytochrome c release from mitochondria: All or nothing. *Nat. Cell Biol.*, 2: E41-E43.
13. Zhang, H., L. Zhai, T. Wang, S. Li and Y. Guo, 2017. Picoside II exerts a neuroprotective effect by inhibiting the mitochondria cytochrome C signal pathway following ischemia reperfusion injury in rats. *J. Mol. Neurosci.*, 61: 267-278.
14. Longa, E.Z., P.R. Weinstein, S. Carlson and R. Cummins, 1989. Reversible middle cerebral artery occlusion without craniectomy in rats. *Stroke*, 20: 84-91.
15. Brancho, D., N. Tanaka, A. Jaeschke, J.J. Ventura and N. Kelkar *et al.*, 2003. Mechanism of p38 MAP kinase activation *in vivo*. *Genes Dev.*, 17: 1969-1978.
16. Kuang, S.Q., O. Medina-Martinez, D.C. Guo, L. Gong and E.S. Regalado *et al.*, 2016. *FOXE3* mutations predispose to thoracic aortic aneurysms and dissections. *J. Clin. Invest.*, 126: 948-961.
17. Wang, T., L. Zhai, H. Zhang, L. Zhao and Y. Guo, 2015. Picoside II inhibits the MEK-ERK1/2-COX2 signal pathway to prevent cerebral ischemic injury in rats. *J. Mol. Neurosci.*, 57: 335-351.
18. Zhao, L., Y.L. Guo, X.J. Ji and M.Z. Zhang, 2014. The neuroprotective effect of picoside II via regulating the expression of myelin basic protein after cerebral ischemia injury in rats. *BMC Neurosci.*, Vol. 15. 10.1186/1471-2202-15-25.
19. Zhao, L., T. Wang, Y. Zhou, X. Li, D. Wang and Y. Guo, 2015. Improvement in the ultrastructures of nervous tissues damaged in cerebral ischemic rate by picoside II. *Int. J. Pharmacol.*, 11: 50-55.
20. Li, S., T. Wang, L. Zhai, K. Ge, J. Zhao, W. Cong and Y. Guo, 2018. Picoside II exerts a neuroprotective effect by inhibiting mPTP permeability and EndoG release after cerebral ischemia/reperfusion injury in rats. *J. Mol. Neurosci.*, 64: 144-155.
21. Levine, A.J., 1997. P53, the cellular gatekeeper for growth and division. *Cell*, 88: 323-331.
22. Milczarek, G.J., J. Martinez and G.T. Bowden, 1997. p53 phosphorylation: Biochemical and functional consequences. *Life Sci.*, 60: 1-11.
23. Durukan, A. and T. Tatlisumak, 2007. Acute ischemic stroke: Overview of major experimental rodent models, pathophysiology and therapy of focal cerebral ischemia. *Pharmacol. Biochem. Behav.*, 87: 179-197.
24. Yan, J., M. Zheng and D. Zhang, 2014. Chrysophanol liposome preconditioning protects against cerebral ischemia-reperfusion injury by inhibiting oxidative stress and apoptosis in mice. *Int. J. Pharmacol.*, 10: 55-68.
25. Li, Q., Z. Li, X.Y. Xu, Y.L. Guo and F. Du, 2010. Neuroprotective properties of picoside II in a rat model of focal cerebral ischemia. *Int. J. Mol. Sci.*, 11: 4580-4590.
26. Wu, N., W. Li, W. Shu and D. Jia, 2014. Protective effect of picoside II on myocardial ischemia reperfusion injury in rats. *Drug Des. Dev. Ther.*, 8: 545-554.
27. Marzo, I., C. Brenner, N. Zamzami, S.A. Susin and G. Beutner *et al.*, 1998. The permeability transition pore complex: A target for apoptosis regulation by caspases and Bcl-2-related proteins. *J. Exp. Med.*, 187: 1261-1271.
28. Azarashvili, T., O. Krestinina, Y. Baburina, I. Odinokova and V. Akatov *et al.*, 2016. Effect of the CRAC peptide, VLNYYVW, on mPTP opening in rat brain and liver mitochondria. *Int. J. Mol. Sci.*, Vol. 17. 10.3390/ijms17122096.

29. Garrido, C., L. Galluzzi, M. Brunet, P.E. Puig, C. Didelot and G. Kroemer, 2006. Mechanisms of cytochrome *c* release from mitochondria. *Cell Death Differ.*, 13: 1423-1433.
30. Dagher, P.C., 2004. Apoptosis in ischemic renal injury: Roles of GTP depletion and p53. *Kidney Int.*, 66: 506-509.
31. Culmsee, C., X. Zhu, Q.S. Yu, S.L. Chan and S. Camandola *et al*, 2001. A synthetic inhibitor of p53 protects neurons against death induced by ischemic and excitotoxic insults and amyloid β -peptide. *J. Neurochem.*, 77: 220-228.
32. Leker, R.R., M. Aharonowiz, N.H. Greig and H. Ovadia, 2004. The role of p53-induced apoptosis in cerebral ischemia: Effects of the p53 inhibitor pifithrin α . *Exp. Neurol.*, 187: 478-486.
33. Khoo, K.H., K.K. Hoe, C.S. Verma and D.P. Lane, 2014. Drugging the p53 pathway: Understanding the route to clinical efficacy. *Nat. Rev. Drug Discov.*, 13: 217-236.
34. Chipuk, J.E., T. Kuwana, L. Bouchier-Hayes, N.M. Drain, D.D. Newmeyer, M. Schuler and D.R. Green, 2004. Direct activation of Bax by p53 mediates mitochondrial membrane permeabilization and apoptosis. *Science*, 303: 1010-1014.
35. Mihara, M., S. Erster, A. Zaika, O. Petrenko, T. Chittenden, P. Pancoska and U.M. Moll, 2003. P53 has a direct apoptogenic role at the mitochondria. *Mol. Cell*, 11: 577-590.